

Catalytic Solvolytic and Hydrolytic Degradation of Toxic Methyl Paraoxon with La(catecholate)-Functionalized Porous Organic Polymers

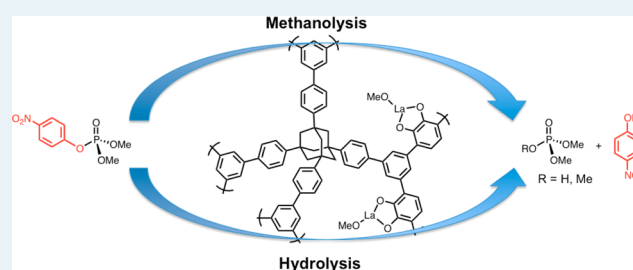
Ryan K. Totten, Mitchell H. Weston, Jin Kuen Park, Omar K. Farha,* Joseph T. Hupp,* and SonBinh T. Nguyen*

Department of Chemistry and the International Institute for Nanotechnology, Northwestern University, 2145 Sheridan Road, Evanston, Illinois 60208-3113, United States

S Supporting Information

ABSTRACT: Two robust catechol-functionalized porous organic polymers (catPOPs) with different T_d -directing nodes were synthesized using a cobalt-catalyzed acetylene trimerization (CCAT) strategy. Postsynthesis metallation was readily carried out with $\text{La}(\text{acac})_3$ to afford catalytically active La-functionalized catPOPs for the solvolytic and hydrolytic degradation of the toxic organophosphate compound methyl paraoxon, a simulant for nerve agents.

KEYWORDS: porous organic polymers, catechol, catalysis, organophosphates, lanthanum



INTRODUCTION

Over the past decade, porous organic polymers (POPs) have emerged as a new class of materials with promising applications in gas storage,^{1–7} chemical separation,^{3,8–11} and heterogeneous catalysis.^{12–17} The directed assembly of one or more rigid organic building blocks into a microporous network using stable organic bonds can afford chemically and thermally stable materials with both highly accessible internal surface areas and a wide range of chemical functionalities.⁷ Of particular interest to us is the design of POPs suitable for applications that combine molecular recognition and catalysis. Specifically, the integration of coordinatively unsaturated metal ions into POPs should afford micropore environments that are capable of binding and transforming small-molecule substrates.¹⁷ Together with the known ability of nanometer-sized cavities to sequester reactants and enhance their in-pore concentrations beyond that in solution,^{18,19} this should lead to enhanced catalysis.

While metal ions have been incorporated into POPs possessing bipyridyl ligands and used for catalysis,^{16,20} this strategy necessitates the use of charge-compensating anions, which can fill valuable pore volumes and block coordination sites.^{12,13,15,16} To generate POPs that can stabilize metal ions featuring high degrees of unsaturation, we have focused instead on the use of negatively charged ligands as building blocks. In addition to porphyrin-based systems,¹³ we have been able to integrate catechol-bearing building blocks into POPs and successfully form POP-stabilized monocatecholated metal complexes with a series of divalent metals (Cu^{II} , Mg^{II} , Mn^{II} , and Zn^{II}) that demonstrate enhanced hydrogen sorption capabilities²¹ and removal of toxic chemicals.²² The dianionic catecholate ligands offset the cationic charges of divalent metal

ions while their isolation inside the POP micropore precludes the formation of stable bis- and tris-chelation motifs that are the dominant species in a homogeneous environment.²³ The result is metal centers with empty or labile coordination environments (solvents or water) that can be used to bind and recognize small molecules.

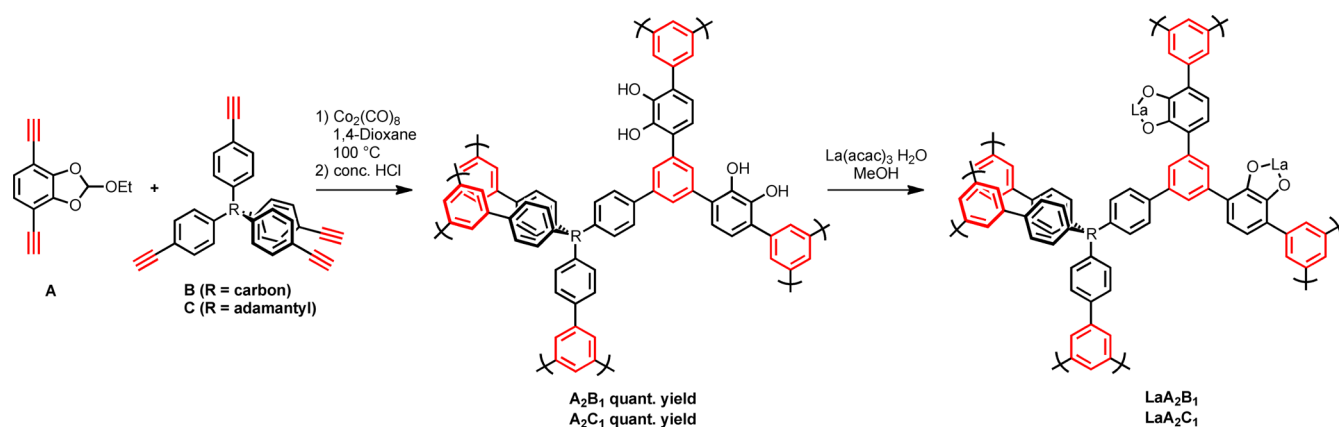
Given our interest in the solvolytic degradation of phosphate triesters and its relevance in the decomposition of toxic organophosphate-based nerve agents,^{19,24} we reasoned that a Lewis-acidic metal ion bound inside a catechol-functionalized POP would be a potent, reusable catalyst for these reactions.^{25,26} While both Al^{III} and Zn^{II} complexes have been used in the supramolecularly catalyzed methanolysis of phosphate esters,^{19,24} we choose to incorporate La^{III} ions into our catechol POPs (catPOP) given its strong oxophilic nature and its ability to coordinate up to 9 ligands.²⁷ We hypothesized that (monocatecholate)La moieties stabilized inside a POP cavity would be able to bind phosphate triesters together with a large number of hydroxylated reagents, such as methanol and water, inside a micropore and accelerate its solvolytic decomposition. In addition to the dianionic catecholate ligand, the third anionic ligand of the La^{III} ion (i.e., MeO^- or HO^-) or other protonated ligands (MeOH or H_2O) can serve as a pool of nucleophiles in the solvolysis/hydrolysis of the coordinated phosphate ester. We note that the high activity of La^{III} ion in the hydrolytic cleavage of DNA²⁸ and solvolysis of phosphate triesters,^{29–31} has been demonstrated.

Received: March 4, 2013

Revised: April 7, 2013

Published: April 15, 2013

Scheme 1. Synthesis of Catechol-Containing POPs A_2B_1 and A_2C_1 Using a Cobalt-Catalyzed Acetylene Trimerization Strategy (CCAT) and Their Subsequent Metallation with La^{III} Ions^a



^aThe POPs shown above are idealized representations of a completely formed network. However, different substitution patterns (1,3,4 vs 1,3,5) may be present as well as olefins/dienes and unreacted acetylene groups because of incomplete polymerization. For the A_2B_1 composition, solid-state ^{13}C NMR analysis suggested that this material is free of olefin/diene groups. See the Supporting Information by Weston et al.²¹ for additional discussion.

2. EXPERIMENTAL SECTION

Synthesis of Polymers. POP A_2B_1 was synthesized following a previously reported procedure.²¹

POP A_2C_1 . In a nitrogen-filled glovebox, a 5 mL microwave vial (capacity designates the amount of solution that can be safely loaded) equipped with a magnetic stir bar was charged with monomers A^{32} (38 mg, 0.18 mmol) and C^{33} (54 mg, 0.09 mmol) in the same optimal ratio found for A_2B_1 .²¹ This mixture was dissolved in dry 1,4-dioxane (4 mL) and $Co_2(CO)_8$ (30 mg, 0.09 mmol) was added. The solution was stirred for 5 min prior to being sealed and removed from the glovebox. The reaction mixture was then stirred at 110 °C in a silicone oil bath for 3 h, during which time a black precipitate formed. Upon cooling to room temperature, the microwave vial was opened and the precipitate was isolated by filtration, washed with H_2O (30 mL), and stirred in conc. aqueous hydrochloric acid (10 mL) for 2 h. The remaining black polymer was filtered, washed with H_2O (30 mL) and MeOH (30 mL), dried over dynamic vacuum, and activated under a stream of nitrogen at 150 °C for 12 h to afford A_2C_1 (80 mg, 97%).

Representative Procedure for the Metallation of Polymers. POP LaA_2B_1 . A_2B_1 (100 mg) was added to a solution of $La(acac)_3 \cdot H_2O$ (260 mg, 0.57 mmol) in MeOH (10 mL) and stirred at 50 °C for 18 h. The suspension was filtered and the solid polymer was extracted for 12 h with MeOH using a Soxhlet apparatus. The remaining material was filtered and activated under a stream of nitrogen at 150 °C for 12 h.

Representative Procedure for the Methanolysis of *p*-nitrophenyl Dimethyl Phosphate (PNPDMP) by La-(catecholate)-Functionalized POPs under Shaking Conditions. On the benchtop, a 2 dram vial was charged with PNPDMP (19 mg, 25 mM), La(catecholate)-functionalized POP catalyst (4 mg for LaA_2C_1 , 6 mol % La^{III}), and methanol (3 mL). The reaction vial was sealed with a Teflon-lined cap and allowed to shake at 200 rpm (see section S5 in the SI for a discussion on the importance of this protocol) and 60 °C in a Thermolyne Type 17600 aluminum heating block (Thermolyne, Dubuque, IA) mounted on a Thermolyne Type 65800 shaker (Thermolyne, Dubuque, IA). Periodically, the reaction vial was removed from the shaker, cooled down to below 50 °C

with a quick spray of acetone (~5 s) to prevent excessive MeOH evaporation, and quickly opened for aliquot (100 μ L) sampling before being put back on the shaker. The sampled aliquot was diluted with MeOH to 25 mL in a volumetric flask and analyzed by UV-vis spectroscopy. The conversion of PNPDMP as a function of reaction time was obtained by monitoring the increase of absorbance of *p*-nitrophenol at 311 nm.

Hydrolysis of *p*-Nitrophenyl Dimethyl Phosphate (PNPDMP) by LaA_2C_1 under Shaking Conditions. On the benchtop, PNPDMP (19 mg, 25 mM), LaA_2C_1 (4 mg, 6 mol % La^{III}) and 4-ethylmorpholine buffer solution (93 mM, 30 vol % EtOH, pH 10, 3 mL)³⁴ were placed in a 2 dram vial. The reaction vial was sealed with a Teflon-lined cap and allowed to shake at 200 rpm and 60 °C in a Thermolyne Type 17600 aluminum heating block (Thermolyne, Dubuque, IA) mounted on a Thermolyne Type 65800 shaker (Thermolyne, Dubuque, IA). Periodically, the reaction vial was removed from the shaker and quickly opened for aliquot (100 μ L) sampling before being put back on the shaker. The sampled aliquot was diluted with the buffer solution to 25 mL in a volumetric flask and analyzed by UV-vis spectroscopy. The conversion of PNPDMP as a function of reaction time was obtained by monitoring the increase of absorbance of the *p*-nitrophenolate ion at 406 nm.

3. RESULTS AND DISCUSSION

In exploring the use of La-functionalized catPOPs for phosphate ester hydrolysis, we wanted to investigate how the substrate accessibility of the micropore reaction environment, and thus its catalytic activity, can be tuned by incorporating different organic linkers. Previously,²¹ we have demonstrated that the copolymerization of an orthoester-protected 1,4-diethynyl-2,3-dihydroxybenzene³⁵ (see Scheme S1 in the SI for its synthesis) with a T_d -directing *tetrakis*(4-ethynyl)methane monomer³⁶ (see Scheme S2 in the SI for its synthesis) in different monomer ratios resulted in a family of porous polymers with tunable surface areas and pore size distributions. One member of this family (A_2B_1 , Scheme 1, R = Carbon,) was then metallated with divalent metals that readily bind small molecules such as H_2 .²¹ For the degradation of large phosphate ester substrates, we hypothesized that using the larger T_d -

Table 1. Pore, Surface, and Catalytic Properties of Catechol-Containing POPs

| entry | POP | BET surface area (m ² /g) | theoretical metal loading (wt %) | actual metal loading (wt %) | total pore volume (cm ³ /g) | dominant pore diameter (Å) | observed initial rate (M s ⁻¹) ^{a,b} | relative initial rate vs uncatalyzed reaction ^c |
|-------|---------------------------------|--------------------------------------|----------------------------------|-----------------------------|--|----------------------------|---|--|
| 1 | A ₂ B ₁ | 1050 | | | 0.51 | 12 ± 2 | | |
| 2 | LaA ₂ B ₁ | 265 | 23 | 22 | 0.09 | 11 ± 2 | 7.0 × 10 ⁻⁷ | 41 |
| 3 | A ₂ C ₁ | 1165 | | | 0.59 | 13 ± 2 | | |
| 4 | LaA ₂ C ₁ | 650 | 20 | 16 | 0.28 | 11 ± 2 | 1.7 × 10 ⁻⁶ | 100 |

^aReaction conditions: PNPDM (25 mM), [La^{III}] (1.5 mM, 6 mol %), MeOH, 60 °C. ^bInitial rates were measured up to 10% conversion and corrected against background reactions. ^cReaction conditions for the uncatalyzed reaction: PNPDM (25 mM), MeOH, 60 °C. Initial rate was also measured up to 10% conversion.

directing *tetrakis*(4-ethynyl)adamantyl monomer³⁷ (Scheme 1, R = adamantyl; see Scheme S3 in the SI for its synthesis) would result in a POP with higher surface area, more accessible pores, and thus increased catalytic activity. In addition, the more hydrophobic adamantyl node could further enhance the solvophobic encapsulation of the hydrophobic PNPDM substrate in polar media and increase the catalysis rate.^{19,24}

As shown in Table 1, polymer A₂C₁ has a BET surface area that is about 10% higher than that for A₂B₁ (1165 vs 1050 m²/g, respectively; see also Figure 1). Both catPOPs were smoothly

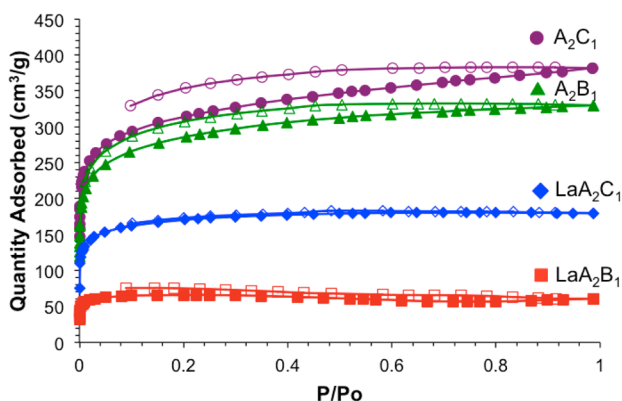


Figure 1. Nitrogen isotherms measured at 77 K for polymers A₂C₁ (purple circles), A₂B₁ (green triangles), LaA₂C₁ (blue diamonds), and LaA₂B₁ (red squares). Closed symbols, adsorption; open symbols, desorption.

metallated in the presence of excess La(acac)₃ to afford the corresponding La-functionalized catPOPs with close to a 1:1 catechol:metal stoichiometry. Although the nonmetallated POPs show a small difference in BET surface areas, LaA₂C₁ shows a surprisingly ~2.5-fold higher surface area over LaA₂B₁ (650 vs 265 m²/g) and a 3-fold higher methanol uptake at 0.80 P_(partial)/P_(relative) (Figure S18 in SI). Given that the pore diameters are similar for both materials, (Figures S14 and S15 in the SI, pore size distributions were calculated using nitrogen and argon measurements respectively) the larger surface area and methanol-uptake capacity for LaA₂C₁ indicate its greater pore accessibility, which should make it a better catalyst for the solvolysis/hydrolysis of a phosphate triester.

The methanolysis of *p*-nitrophenyl dimethyl phosphate (PNPDMP), a toxic pesticide and simulant for chemical warfare agents,³⁸ is enhanced by both LaA₂B₁ and LaA₂C₁ (Figure 2). As expected, significantly enhanced activity was observed with POP LaA₂C₁, which has much higher specific surface area than LaA₂B₁: the initial methanolysis rate for the former is ~2.5 fold faster than that for the latter (Table 2). Surprisingly, a significant amount of La^{III} (10% of the overall

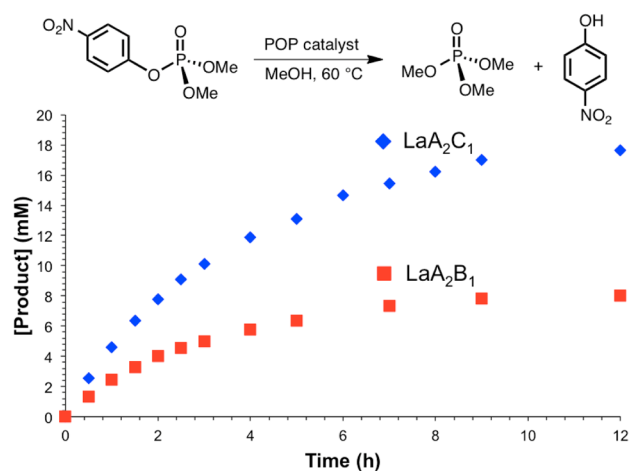


Figure 2. Reaction profiles for the methanolysis of PNPDM in the presence of 6 mol % of either LaA₂C₁ (blue diamonds) or LaA₂B₁ (red squares).

Table 2. Observed Initial Rates in the Methanolysis of PNPDM by LaA₂B₁ and LaA₂C₁

| catalyst ^a | cycle | observed initial rate (M s ⁻¹) ^b | La ^{III} leaching (%) ^c | relative rate vs uncatalyzed reaction |
|---------------------------------|----------------|---|---|---------------------------------------|
| LaA ₂ B ₁ | 1 | 7.0 × 10 ⁻⁷ | 10.1 | 41 |
| LaA ₂ C ₁ | 1 | 1.7 × 10 ⁻⁶ | 0.1 | 100 |
| | 2 | 7.1 × 10 ⁻⁷ | 0.6 | 42 |
| | 3 | 2.9 × 10 ⁻⁷ | 4.3 | 17 |
| | 4 ^d | 7.0 × 10 ⁻⁸ | 1.4 | 4 |

^aReaction conditions: PNPDM (25 mM), [La^{III}] (1.5 mM, 6 mol %), MeOH, 60 °C. ^bInitial rates were measured up to 10% conversion and corrected against background reactions. ^cPercentage of the initial metal loading. ^dAfter Soxhlet extraction with THF.

La^{III} content as determined by ICP-OES analysis of the product solutions) leached from LaA₂B₁ during the reaction, in contrast to the negligible leaching in the case of LaA₂C₁ (Table 2). Although the BET-derived pore size distributions of these two materials are quite similar (Figures S14 and S15 in the SI), the leaching differences can be explained if the local environments around the La(catecholate) moieties are different enough to cause instability. Supporting this speculation is the observation that the acac counterion is not visible in the solid-state IR spectra of LaA₂B₁, but is observable in that for LaA₂C₁ (see section S13 in the SI).

The degree of La^{III} leaching was further corroborated by monitoring the catalytic activities of the solution phases in the methanolysis of PNPDM by LaA₂C₁ and LaA₂B₁. After each reaction reached 30% conversions (~2 h for LaA₂C₁ and ~3 h

for LaA_2B_1), the POP particles were removed by filtering and the PNPDMMP concentrations in the solutions were further monitored. The background-corrected rate of methanolysis is ~ 1.7 -fold higher in the filtrate for LaA_2B_1 than that for LaA_2C_1 (Figure S12 in the SI), which is consistent with the former containing a larger amount of leached La^{III} ions. The activity in the filtrate is much less than that for an equivalent amount of $\text{La}(\text{acac})_3$ (see section S6 in the SI), suggesting that the leached La^{III} is a much less-active form than $\text{La}(\text{acac})_3$ monomer.

Motivated by the promising catalytic activity of LaA_2C_1 , we examined its recyclability in the methanolysis of PNPDMMP (Table 2). Surprisingly, the initial methanolysis rate drops significantly with each cycle, even though little leaching of La^{III} is observed. This phenomenon can be attributed to a number of factors: (1) the substrate/products are retained in the pores during catalysis, thus blocking new substrate from entering; (2) the framework of the POP is degraded/relaxed, which inhibits substrate access to the catalytic sites;³⁹ or (3) the encapsulated $\text{La}(\text{catecholate})$ moieties are degraded into less-active forms during catalysis.

To evaluate the possibility that substrate/products may be clogging the pores, LaA_2C_1 was Soxhlet-extracted with THF for 24 h after the third cycle. Surprisingly, evaluation of the filtrate by UV-vis spectroscopy revealed a significant amount of “adsorbed” PNPDMMP substrate (2.7 mg from 6.6 mg of isolated materials, or a 2.4 substrate:La molar ratio). While we cannot determine if the adsorbed substrate is bound to the oxophilic La^{III} ion, its sequestration in the pores might be limiting transport between the pores and the external solution, thereby contributing to the reduction of catalytic activity. Unfortunately, the catalytic activity of the Soxhlet-extracted LaA_2C_1 did not improve, as the initial rate for the “fourth” cycle was only 4 \times faster than that for the uncatalyzed reaction.

To evaluate factors 2 and 3, we “aged” LaA_2C_1 in methanol at 60 °C and in the absence of PNPDMMP for four days, and then remeasured its surface area by N_2 gas adsorption (see Section S8 in the SI). To our surprise, the BET surface area greatly decreased (650 m^2/g as-synthesized vs 180 m^2/g aged, Figure 3). However, conducting the same aging experiment on the nonmetallated POP A_2C_1 produced no significant change in surface area (1170 m^2/g as-synthesized vs 1080 m^2/g aged). This result led us to conclude that the degradation of supported $\text{La}(\text{catecholate})$ moieties into less-active forms must be an important contributor to the successive decrease in catalysis rate. Although we do not know the exact nature of the

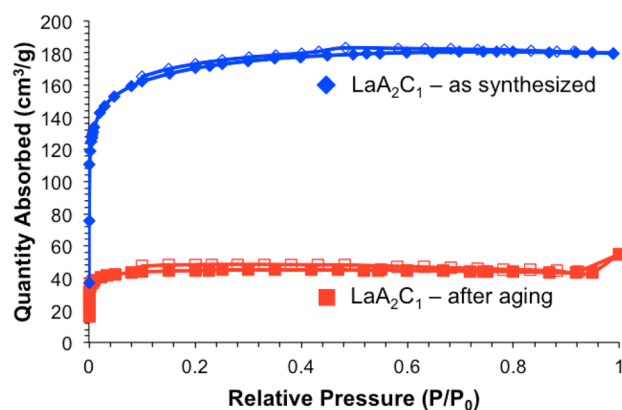


Figure 3. BET isotherms for as-synthesized LaA_2C_1 (blue diamonds) and after aging (red squares) at 60 °C in methanol for four days.

degradation products, it is conceivable that the La^{III} ion could be cleaved from the catechol in the presence of MeOH to form less active species that are trapped in the micropores. Such an explanation is consistent with both the low La^{III} leaching and the decrease in the surface area of the POP. Together with the build-up of substrate in the pores, these data indicate that the drop in catalytic activity after each cycle of methanolysis is due to a combination of $\text{La}(\text{catecholate})$ degradation as well as a decrease in transport through the pores of LaA_2C_1 because of substrate sequestration.

As both A_2C_1 and LaA_2C_1 can take up a significant amount of water vapor (see Figure S19 in SI, section 14), we hypothesize that LaA_2C_1 would be active in the hydrolysis of PNPDMMP, which is a more practical route toward the destruction of nerve agents.⁴⁰ Under pH 10 buffered conditions and in 30 vol % EtOH, which helps to solubilize the nerve agent simulant, the hydrolysis of PNPDMMP in the presence of LaA_2C_1 is 12 times faster than the uncatalyzed reaction (Figure 4). In contrast to the catalyzed methanolysis of PNPDMMP,

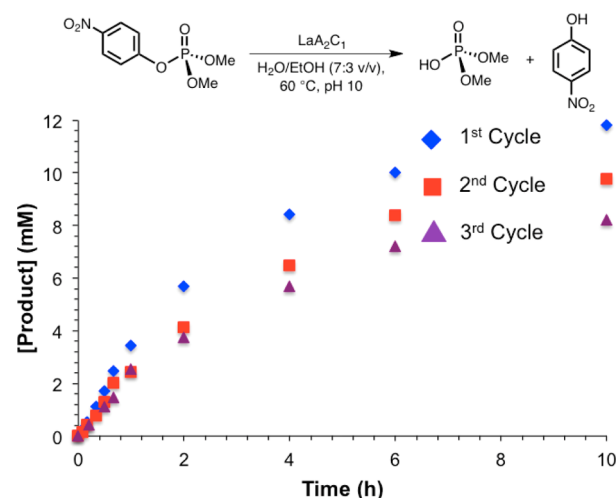


Figure 4. Reaction profiles for the first three hydrolysis cycles of PNPDMMP in the presence of 6 mol % LaA_2C_1 in 4-ethyl morpholine buffer solution (93 mM, 30 vol % EtOH, pH 10) using shaking conditions. First cycle, blue diamonds; second cycle, red squares; third cycle, purple triangles.

LaA_2C_1 retains significantly more catalytic activity over three cycles of hydrolysis: the initial rate only drops 40% after the first cycle and remains the same for the second and third cycles, showing good recyclability (Table 3). Soxhlet extraction of the LaA_2C_1 catalyst after each cycle revealed essentially no trapping

Table 3. Observed Initial Rates in the Hydrolysis of PNPDMMP by LaA_2B_1 and LaA_2C_1

| catalyst ^a | cycle | observed rate (M s^{-1}) ^b | La^{III} leaching (%) ^c | relative rate vs uncatalyzed reaction |
|--------------------------|-------|--|--|---------------------------------------|
| LaA_2B_1 | 1 | 1.1×10^{-6} | 0.1 | 12 |
| LaA_2C_1 | 1 | 1.1×10^{-6} | 0.1 | 12 |
| | 2 | 6.7×10^{-7} | 0.1 | 7 |
| | 3 | 6.7×10^{-7} | 0.2 | 7 |

^aReaction conditions: PNPDMMP (25 mM), $[\text{La}^{\text{III}}]$ (1.5 mM, 6 mol %), 4-ethyl morpholine buffer solution (93 mM, 30 vol % EtOH, pH 10), 60 °C. ^bInitial rates were measured up to 10% conversion and corrected against background reactions. ^cPercentage of the initial metal loading.

of the substrate (see section S11 in the SI) and the amount of La leaching from LaA_2C_1 is again negligible. Together, these data suggest that under the basic buffered aqueous conditions, transport of the substrates through the cavities of LaA_2C_1 is more facile and the La^{III} sites are more stable against decomposition. The basic aqueous environment of the solution must have preferentially solubilized both the substrate and the acidic hydrolyzed products, keeping them from clogging the pores. Interestingly, PNPDPMP hydrolysis by LaA_2B_1 under the same conditions yields similar turnover number with minimal leaching (Table 3).

4. SUMMARY AND CONCLUSIONS

In summary, two robust catechol-functionalized POPs with different T_{d} -directing nodes can be synthesized and metallated with La^{III} ions to afford catalytically active materials for the solvolytic and hydrolytic degradation of toxic organophosphates. Most notably, POP LaA_2C_1 , with its higher accessible surface area, has significantly enhanced rates in the methanolytic decomposition of PNPDPMP relative to the carbon-noded POP LaA_2B_1 . Presumably, the higher specific surface area of the former increases its pore accessibility to the substrates and thus increases reaction rates. While there is minimal leaching of La^{III} ions from the pores of POP LaA_2C_1 , La(catecholate) degradation appears to be more significant in methanol; the significant decrease in methanolysis rate of LaA_2C_1 after each recycling experiment can, in part, be attributed to this problem. In addition, the choice of reaction media is an important consideration in the decomposition of PNPDPMP: when the external medium does not solvate this substrate and its products well, preferential sequestration of these species inside the pores can clog them and significantly reduce catalysis. Clearly, one needs to keep in mind parameters such as pore accessibility and reaction media in the design of new catalyst materials.

■ ASSOCIATED CONTENT

■ Supporting Information

Complete procedures for the synthesis of POP starting materials and characterization data (FTIR, ^1H , and ^{13}C NMR), H_2O and MeOH vapor isotherms and pore size distribution graphs, detailed procedures for catalysis, aging experiments, and the determination of nitrophenol extinction coefficient. This material is available free of charge via the Internet at <http://pubs.acs.org>.

■ AUTHOR INFORMATION

■ Corresponding Author

*E-mail: o-farha@northwestern.edu (O.K.F.); j-hupp@northwestern.edu (J.T.H.); stn@northwestern.edu (S.T.N.).

■ Notes

The authors declare no competing financial interest.

■ ACKNOWLEDGMENTS

Financial support for this work is provided by DTRA (agreement HDTRA1-10-1-0023). Instruments in the Northwestern University Integrated Molecular Structure Education and Research Center (IMSERC) were purchased with grants from NSF-NSEC, NSF-MRSEC, Keck Foundation, the state of Illinois, and Northwestern University.

■ REFERENCES

- (1) Weber, J.; Thomas, A. *J. Am. Chem. Soc.* **2008**, *130*, 6334–6335.
- (2) Ben, T.; Ren, H.; Ma, S.; Cao, D.; Lan, J.; Jing, X.; Wang, W.; Xu, J.; Deng, F.; Simmons, J. M.; Qiu, S.; Zhu, G. *Angew. Chem., Int. Ed.* **2009**, *48*, 9457–9460.
- (3) Chen, Q.; Luo, M.; Hammershøj, P.; Zhou, D.; Han, Y.; Laursen, B. W.; Yan, C.-G.; Han, B.-H. *J. Am. Chem. Soc.* **2012**, *134*, 6084–6087.
- (4) Cooper, A. I. *Adv. Mater.* **2009**, *21*, 1291–1295.
- (5) Yuan, D.; Lu, W.; Zhao, D.; Zhou, H.-C. *Adv. Mater.* **2011**, *23*, 3723–3725.
- (6) Rabbani, M. G.; El-Kaderi, H. M. *Chem. Mater.* **2011**, *23*, 1650–1653.
- (7) Hauser, B. G.; Farha, O. K.; Exley, J.; Hupp, J. T. *Chem. Mater.* **2012**, *25*, 12–16.
- (8) Farha, O. K.; Spokoyny, A. M.; Hauser, B. G.; Bae, Y.-S.; Brown, S. E.; Snurr, R. Q.; Mirkin, C. A.; Hupp, J. T. *Chem. Mater.* **2009**, *21*, 3033–3035.
- (9) McKeown, N. B.; Budd, P. M. *Chem. Soc. Rev.* **2006**, *35*, 675–683.
- (10) Rabbani, M. G.; El-Kaderi, H. M. *Chem. Mater.* **2012**, *24*, 1511–1517.
- (11) Peterson, G. W.; Farha, O. K.; Schindler, B.; Jones, P.; Mahle, J.; Hupp, J. T. *J. Porous Mater.* **2012**, *19*, 261–266.
- (12) Mackintosh, H. J.; Budd, P. M.; McKeown, N. B. *J. Mater. Chem.* **2008**, *18*, 573–578.
- (13) Shultz, A. M.; Farha, O. K.; Hupp, J. T.; Nguyen, S. T. *Chem. Sci.* **2011**, *2*, 686–689.
- (14) Zhang, Y.; Riduan, S. N. *Chem. Soc. Rev.* **2012**, *41*, 2083–2094.
- (15) Xie, Z.; Wang, C.; deKrafft, K. E.; Lin, W. *J. Am. Chem. Soc.* **2011**, *133*, 2056–2059.
- (16) Jiang, J.-X.; Wang, C.; Laybourn, A.; Hasell, T.; Clowes, R.; Khimyak, Y. Z.; Xiao, J.; Higgins, S. J.; Adams, D. J.; Cooper, A. I. *Angew. Chem., Int. Ed.* **2011**, *50*, 1072–1075.
- (17) Kaur, P.; Hupp, J. T.; Nguyen, S. T. *ACS Catal.* **2011**, *1*, 819–835.
- (18) Shultz, A. M.; Farha, O. K.; Hupp, J. T.; Nguyen, S. T. *J. Am. Chem. Soc.* **2009**, *131*, 4204–4205.
- (19) Kang, B.; Kurutz, J. W.; Youm, K.-T.; Totten, R. K.; Hupp, J. T.; Nguyen, S. T. *Chem. Sci.* **2012**, *3*, 1938–1944.
- (20) Wang, J.-L.; Wang, C.; deKrafft, K. E.; Lin, W. *ACS Catal.* **2012**, *2*, 417–424.
- (21) Weston, M. H.; Farha, O. K.; Hauser, B. G.; Hupp, J. T.; Nguyen, S. T. *Chem. Mater.* **2012**, *24*, 1292–1296.
- (22) Weston, M. H.; Peterson, G. W.; Browe, M. A.; Jones, P.; Farha, O. K.; Hupp, J. T.; Nguyen, S. T. *Chem. Commun.* **2013**, *49*, 2995–2997.
- (23) Pierpont, C. G.; Lange, C. *Prog. Inorg. Chem.* **2007**, *41*, 331–442.
- (24) Totten, R. K.; Ryan, P.; Kang, B.; Lee, S. J.; Broadbelt, L. J.; Snurr, R. Q.; Hupp, J. T.; Nguyen, S. T. *Chem. Commun.* **2012**, *48*, 4178–4180.
- (25) We note that Cohen and coworkers have incorporated protected-catechol struts into a derivative of UMCM-1 de novo, removed the protecting groups, and then metallated the free catechol groups with Fe(II). However, the metallated MOF was not demonstrated for catalytic capability. See: Tanabe, K. K.; Allen, C. A.; Cohen, S. M. *Angew. Chem., Int. Ed.* **2010**, *49*, 9730–9733.
- (26) Parallel work using porous organic polymer (POPs) decorated with catechol groups as supports for unsaturated metal coordination environment with applications in catalysis have been published: (a) Tanabe, K. K.; Siladke, N. A.; Broderick, E. M.; Kobayashi, T.; Goldston, J. F.; Weston, M. H.; Farha, O. K.; Hupp, J. T.; Pruski, M.; Mader, E. A.; Johnson, M. J. A.; Nguyen, S. T. *Chem. Sci.* **2013**, *4*, 2483–2489. (b) Kraft, S. J.; Sánchez, R. H.; Hock, A. S. *ACS Catal.* **2013**, *3*, 826–830.
- (27) Shibasaki, M.; Yoshikawa, N. *Chem. Rev.* **2002**, *102*, 2187–2210.
- (28) Franklin, S. J. *Curr. Opin. Chem. Biol.* **2001**, *5*, 201–208.

- (29) Melnychuk, S. A.; Neverov, A. A.; Brown, R. S. *Angew. Chem., Int. Ed.* **2006**, *45*, 1767–1770.
- (30) Tsang, J. S.; Neverov, A. A.; Brown, R. S. *J. Am. Chem. Soc.* **2003**, *125*, 7602–7607.
- (31) Tsang, J. S. W.; Neverov, A. A.; Brown, R. S. *Org. Biomol. Chem.* **2004**, *2*, 3457–3463.
- (32) Weibel, N.; Błaszczuk, A.; von Hänisch, C.; Mayor, M.; Pobelov, I.; Wandlowski, T.; Chen, F.; Tao, N. *Eur. J. Org. Chem.* **2008**, 136–149.
- (33) Galoppini, E.; Gilardi, R. *Chem. Commun.* **1999**, 173–174.
- (34) Klinkel, K. L.; Kiemele, L. A.; Gin, D. L.; Hagadorn, J. R. *Chem. Commun.* **2006**, 2919–2921.
- (35) This compound was synthesized from commercially available 1,2-dimethoxybenzene (6 steps, 24% overall yield).
- (36) This compound was synthesized from commercially available tetraphenylmethane (3 steps, 41% overall yield).
- (37) This compound was synthesized from commercially available 1-bromoadamantane (4 steps, 50% overall yield).
- (38) Edwards, D. R.; Liu, C. T.; Garrett, G. E.; Neverov, A. A.; Brown, R. S. *J. Am. Chem. Soc.* **2009**, *131*, 13738–13748.
- (39) Pandey, P.; Katsoulidis, A. P.; Eryazici, I.; Wu, Y.; Kanatzidis, M. G.; Nguyen, S. T. *Chem. Mater.* **2010**, *22*, 4974–4979.
- (40) Smith, B. M. *Chem. Soc. Rev.* **2008**, *37*, 470–478.